

## **A STUDY OF THE EMC PERFORMANCE OF A GRADED-IMPEDANCE, MICROWAVE, RICE-HUSK ABSORBER**

**M. N. Iqbal<sup>1, \*</sup>, F. Malek<sup>2</sup>, S. H. Ronald<sup>2</sup>, M. Shafiq<sup>2</sup>,  
K. M. Juni<sup>3</sup>, and R. Chat<sup>3</sup>**

<sup>1</sup>School of Computer and Communication Engineering, Universiti Malaysia Perlis (UniMAP), Taman Seberang Jaya Fasa 3, Kuala Perlis, Perlis 02000, Malaysia

<sup>2</sup>School of Electrical System Engineering, Universiti Malaysia Perlis (UniMAP), Taman Seberang Jaya Fasa 3, Kuala Perlis, Perlis 02000, Malaysia

<sup>3</sup>Electrical Engineering Department, Politeknik Tuanku Syed Sirajuddin, Pauh Putra, Perlis 02600, Malaysia

**Abstract**—Biomass used for energy, whether it is extracted from forest residues or agricultural waste, contributes in many areas, such as power production, the construction industry, and also as a major source of different organic and inorganic compounds in the petrochemical industry. In recent years, research has identified a very remarkable use of agricultural waste, especially rice husks, as a microwave absorber in a pyramidal shape. However, absorbers built in this shape are fragile and require a very high degree of care, especially near the access panels, doors, and high traffic areas of the anechoic facility. This paper presents the results of a detailed experimental investigation of a more-robust, new design that is based on the concept of impedance or dielectric grading of rice-husk material. The absorber was fabricated using multiple layers of rice-husk material with increasing dielectric loss along the incident wave propagation axis. This type of fabrication technique provides more robust design of the microwave, rice-husk absorber with less thickness, as compared to the geometrically-tapered, pyramid, or wedge absorbers. Free-space transmission and radar cross section (RCS) methods have been used, to study the electromagnetic compatibility (EMC) performance over the frequency range of 4–8 GHz. After the receiving equipment was calibrated by

---

*Received 20 July 2012, Accepted 23 August 2012, Scheduled 3 September 2012*

\* Corresponding author: Muhammad Nadeem Iqbal (mr.nadeemiqbal@gmail.com).

the thru-reflect-line (TRL) calibration technique, the experiments were performed inside the anechoic chamber. The performance of the absorber was evaluated by incorporating the effects of circular-hole perforation, cross-polarized seams, and different metallic back plates. The proposed absorber demonstrated good performance ( $< -10$  dB) for normal and  $60^\circ$  off the normal incident angles over the frequency range of 4–8 GHz. Reflectivity performance also was found to be comparable to one of the commercially-available absorbers.

## 1. INTRODUCTION

Rice is the most popular food item throughout the world, and producing the crop contributes a major agricultural waste in the form of rice husks. Rice-husk ash (RHA), another by-product of the rice crop that is obtained after burning rice husks in ferrocement furnaces, has been used as a replacement material for the cement in such furnaces [1]. Rice husks are used in many ways, including cattle feed, fuel for furnaces and gasifiers, and feedstock for chemical, paperboard, and silica industries [2]. However, its effectiveness in electromagnetic energy absorption has been proven in recent years [3]. Rice husks contain high contents of Carbon (35–37%) which is considered as a lossy non-metallic conductor. High surface area and lossy nature of the Carbon help to attenuate the microwaves that pass through the rice husks. Microwave absorbers are used to dampen the cavity resonances, but their most extensive use is in the design of reflectionless environments, such as EMC and antenna measurement anechoic chambers.

In recent years, several semi-anechoic chambers (SACs) and fully-anechoic chambers (FACs) have been designed and fabricated by different manufacturers to simulate the free space environment. With the growth of modern electronics and telecommunication products in medical, commercial, and military command and control systems, demand for electromagnetic compatibility (EMC) chambers with diversity in size and shape has increased significantly. Electronic products must meet both emission and immunity requirements of EMC regulations before they can be advertised in the market [4]. Different regulatory authorities and commissions regulate the EMC issues worldwide. In the United States, the Federal Communications Commission (FCC), and, in Europe, the European Union (EU) regulates the EMC requirements [5].

EMC radiated testing involves radiated emission (RE) testing and radiated susceptibility (RS) testing of the equipment under test (EUT). Each type of testing requires different anechoic chambers,

i.e., RE testing requires an EMC chamber the performance of which is comparable to the open area test site (OATS), whereas uniformity of the electric field is the main issue for RS testing. The power levels of the radiated signals in these tests, especially in case of RS testing, might be dangerous. Therefore, reflectivity-controlled environments, such as reverberation chambers, anechoic chambers, or OATS are necessary to ensure the safety of the personnel and the precision of the results.

The electromagnetic performance of any EMC anechoic chamber depends on the effectiveness of the enclosure's shielding and the reflectivity of the internally-lined absorbers. The highly conductive nature of the shielded enclosure makes it a multi-frequency resonator, and the total field at any position within the anechoic chamber will be the vector sum of the incident and reflected waves. Resonant frequencies depend on the dimensions of the enclosure. The existence of complex, standing-wave patterns can introduce higher-order variability in the field strength at the EUT location [6]. The unwanted resonant environment can be eliminated by the proper selection of absorbing material in the resonant range. At low frequencies, ferrite tiles can be a good option because they provide maximum useable volume, but they are expensive and heavy. Pyramid dielectric absorbers are used at microwave frequencies, and their performance is achieved by absorption through gradual impedance tapering. Tapered impedance ensures the minimum reflection of microwave energy and results in the best performance of absorbers for EMC applications.

Microwave absorption characteristics of the absorber for high-power applications may vary due to the temperature variations that occur due to the heat that is generated [7]. The heat absorbed by the microwave absorbers within the anechoic shielded chambers is usually removed by natural or forced-convection heat transfer. This heat removal depends on the air-absorber contact area and the temperature gradients within the microwave absorber during the heat-transfer process. However, due to the pyramidal geometry of the microwave absorber and the energy distribution of the incident wave, hot spots can occur on its leading tapered edge where less bulk material is present [8]. This will result in impedance mismatches and degradation of the performance of the absorber.

The main concern is the installation of the absorbers inside enclosures, which requires special attention and expertise to minimize the probability of seams. During the installation of the absorbers, it is always possible for a seam or slot to occur between adjacent absorber blocks. Such seams and their orientation with respect to the incident field are very important because they can affect the whole anechoic environment. Incident high-frequency waves can pass through that

seam depending upon their wavelength and orientation, and they will bounce back after striking the wall of the metallic enclosure. These reflected waves will increase the possibility of false signals at the receiving port during EMC testing.

The rice-husk absorber has been investigated by many researchers, but their main focus has been to prove its potential use as a microwave absorber in the pyramidal shape [3]. Currently, it is important to explore its practical applications in actual situations, such as in anechoic chambers. In this experiment, very-simple, planar absorber geometry was used due to ease of its fabrication and robustness of the design as compared to the pyramidal design. The concept of grading dielectric materials was used in this study to investigate the performance of the rice husk. Broadband and better reflectivity ( $< -10$  dB) performance has been achieved by using the proposed impedance grading technique. It is not an easy task to install an absorber in the corners of an enclosure, so most manufacturers design special, miter-joint absorbers for corners. So, it is very important to know the performance of the graded rice-husk material before using any piece of the absorber within the enclosure. In this research, we investigated the absorber by using simple measurement techniques for its future EMC applications inside anechoic chambers. Some relevant theoretical aspects concerning the interface reflections according to the transmission line theory are briefly summarized in Section 2. Then, a detailed description of the EMC characterization of the absorbers is given in Section 3. Section 4 describes the geometrical details of the designed absorbers and comprehensive results are presented in Section 5. A comparison, of the performance of the designed absorbers, with a commercially available absorber is also given in Section 6. Some conclusions are summarized and discussed at the end of the paper.

## 2. INTERFACE REFLECTIONS

Reflection loss at the interface of any two media is related to the impedance mismatch at the interface [9,10]. Matching of both permittivity and permeability of the interface media results in minimum reflection and ensures the maximum absorption of the energy of the incident waves within the lossy medium. The refractive index of the target medium is an important parameter to slow down the incident microwaves within the medium. The refractive index of a rice husk-based absorber is greater than that of air, so microwave signals will be deflected when they enter the absorber [10]. The shape of the dielectric absorbers also plays an important role in minimizing the impedance mismatch by providing smooth impedance tapering of the

target material, which occurs in a microwave-pyramid absorber.

Circuit theory can only be applied to systems that are physically smaller than the wavelength having lumped elements. Since dielectric absorbers act as distributed networks, transmission-line theory can be used at microwave frequencies to explain the scattering of the electromagnetic waves. The technique of “scattering” parameters, commonly called *S*-parameters, relates the reflection and transmission coefficients of the device to the characteristic impedance of the material [5].

2.1. Single Section Transformer and Absorber Analogy

Transmission line theory can be used at high frequencies to explain the analogy of the single-section, quarter-wave-impedance transformer with the quarter-wave-dielectric absorber. Partial reflection and

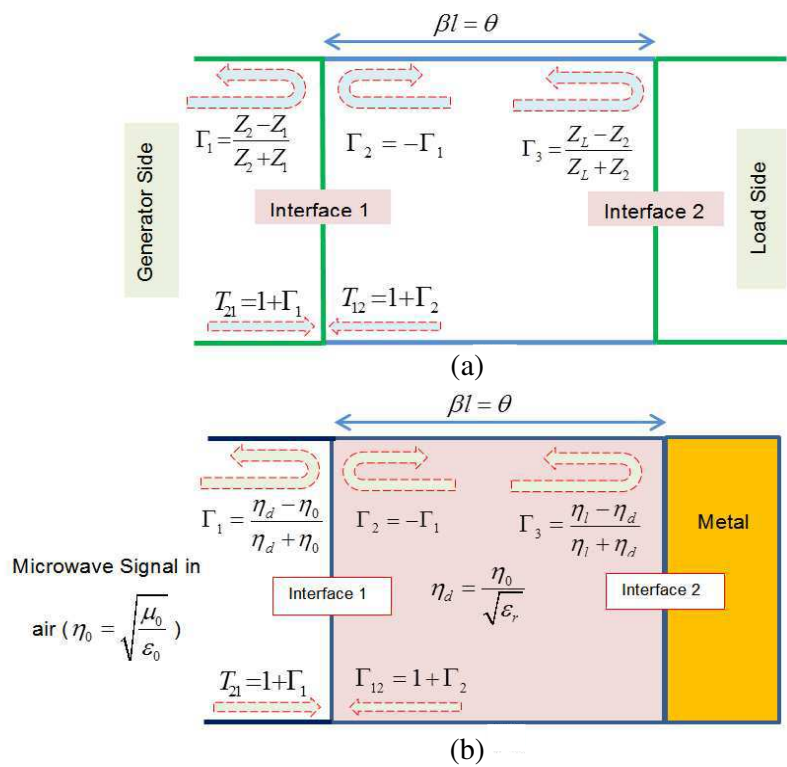


**Figure 1.** Transmission line analogy: (a) Quarter-wave, single-section, impedance transformer. (b) Quarter-wave, single-layer dielectric absorber.

transmission coefficients for both cases are shown in Figure 1.

An infinite number of bouncing waves will exist at interfaces 1 and 2, leading to the total reflection as a sum of all partial reflection and transmission coefficients [10]:

$$\Gamma = \Gamma_1 + T_{12}T_{21}\Gamma_3e^{-2j\theta} + T_{12}T_{21}\Gamma_3^2\Gamma_2 + \dots \quad (1)$$

$$= \Gamma_1 + T_{12}T_{21}\Gamma_3e^{-2j\theta} \sum_{n=0}^{\infty} \Gamma_2^n \Gamma_3^n e^{-2jn\theta}. \quad (2)$$

where  $\theta = \beta l$ , and  $\beta = 2\pi/\lambda$ . Using the geometric series:

$$\sum_{n=0}^{\infty} x^n = \frac{1}{1-x}, \text{ for } |x| < 1 \quad (3)$$

$$\Gamma = \Gamma_1 + \frac{T_{12}T_{21}\Gamma_3e^{-2j\theta}}{1 - \Gamma_2\Gamma_3e^{-2j\theta}} \quad (4)$$

Inserting partial transmission coefficients from Figure 1, we can express the total reflection coefficient as:

$$\Gamma = \frac{\Gamma_1 + \Gamma_3e^{-2j\theta}}{1 + \Gamma_1\Gamma_3e^{-2j\theta}} \quad (5)$$

If the impedance discontinuities at interfaces 1 and 2 are very small, then  $|\Gamma_1\Gamma_3| \ll 1$ , and Equation (5) can be approximated as:

$$\Gamma = \Gamma_1 + \Gamma_3e^{-2j\theta} \quad (6)$$

The total reflection is dominated by the reflection at interface 1 and interface 2, and the term  $e^{-2j\theta}$  accounts for the phase delay. This is analogous to the interaction of the microwave signal with the single-layer, dielectric material that has a characteristic impedance,  $\eta_d = \eta_0/\sqrt{\epsilon_r}$ , and a dielectric constant,  $\epsilon_r$ .

## 2.2. Multi-section Transformer and Graded Multilayers

Step changes in the characteristic impedance between the sections become smaller as the number of discrete sections of the transformer increases. Single-section, quarter-wave impedance transformers and absorbers both provide the minimum reflection response at the design frequency, which results in a narrowband impedance matching. Broadband characteristics of the transformer can be approached by adding an infinite number of discrete sections. Similarly, a narrowband resonant absorber can be converted into a broadband absorber by adding multilayers or by tapering the shape [10,11]. Ideally, infinite layers are required to achieve impedance continuity

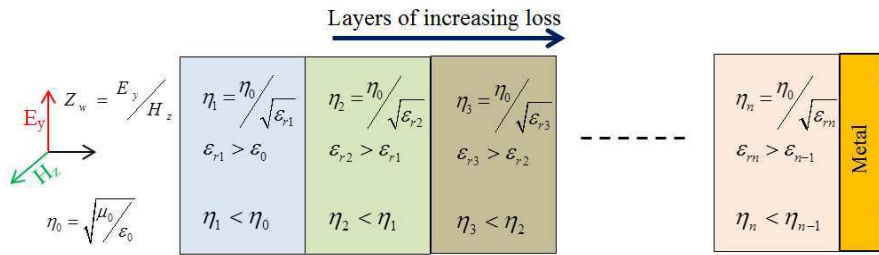


**Figure 2.** Concept of impedance grading with multilayers of increasing loss along signal propagation ( $x$ -axis).

between the successive layers, but, practically, the discontinuity of the impedance only can be minimized to a limited extent. Multilayers with different grades of dielectric properties provide very efficient broadband characteristics if the impedance of each successive layer is kept smooth. Smooth impedance grading will enhance the transmission of the incident wave through each successive layer with smaller reflections at the interface of each layer. However, these small reflections cannot be removed completely due to the step impedance between each layer. Transmitted waves will be reflected an infinite number of times within the multi-layer absorber and lose their energy before reaching the reflecting enclosure wall. The microwave signals lose their energy due to the lossy nature of the absorber, and conversion of electrical energy into heat occurs within the absorber. Figure 2 shows the concept of impedance grading with multilayers of increasing loss.

When the structures are properly designed, the wave that emerges from a geometrically-graded or a material-graded absorber will have a very small amount of energy and cause minimal disturbances to the anechoic environment. If the geometrical or dielectric gradients are so smooth that we can ignore the impedance variations of consecutive layers of the microwave absorber, the theory of small reflections for a multi-section transformer can be used, and total input reflection coefficient can be expressed by Equation (7):

$$\Gamma_{in}(\omega) = \sum_{n=0}^N \Gamma_n e^{-j2n\beta l} \quad (7)$$

### 2.3. Heat Transfer in the Absorber

Microwave interaction with the absorber results in energy dissipation and temperature gradients within the absorber. Heat generation depends on the concentration patterns of electromagnetic energy

at different points. Impurities and non-homogenous mixing of the constituents contribute to the non-uniform concentration of heat within the absorber. However, heat transfer through the thermal conduction process within the absorber limits the accumulation of the dissipated energy [7]. For a steady-state, thermal phenomenon, Fourier's law for thermal power flow  $q$  ( $\text{W}/\text{m}^2$ ) in terms of temperature gradients and thermal conductivity  $k$  ( $\text{W}/\text{m}\cdot^\circ\text{C}$ ) can be expressed as:

$$q = -k\nabla T \quad (8)$$

Transfer of heat from the absorber to the enclosure's environment takes place by convective heat flow. Forced-air cooling is commonly used to remove heat from the absorber.

### 3. CHARACTERIZATION OF THE ABSORBER'S EMC

Characterization of the microwave EMC of the dielectric material involves measuring the relative complex permittivity, and its value must be accurately known to design dielectric microwave absorbers. The effective relative permittivity term is used for absorbers that contain multilayers of non-interacting and distributive constituents [12], and it is given by the expression:

$$\varepsilon_{r,eff} = \frac{\sum_{i=1}^n \varepsilon_{ri} t_i}{\sum_{i=1}^n t_i} \quad (9)$$

where  $\varepsilon_{ri}$  and  $t_i$  represent the dielectric constant and the thickness of the  $i$ th layer, respectively.

There are many experimental techniques that involve either two-port transmission or one-port reflection methods, e.g., waveguides, resonant cavities, and free-space techniques for microwave characterization of this parameter [13]. Some techniques require special machining of the samples before they can be characterized, e.g., rectangular or coaxial waveguides or cavities in which machined samples are inserted [14]. On the other hand, resonant cavities are known to provide high-accuracy measurements for low-loss materials and are limited to a single frequency [15].

#### 3.1. Free-Space Measurement of Complex Permittivity

In this experiment, the free-space, transmission-coefficient measurement technique was used to determine the dielectric properties of the rice-husk absorber. This is a broadband, contactless, non-destructive testing (NDT) technique that does not require specific and accurate



sample machining for microwave characterizations. Measurement of reflection and transmission coefficients can be done simultaneously, and the complex permittivity can be computed from the resulting data [16–20]. However, we used the scattering transmission coefficient method instead of the scattering reflection coefficient. In this simple method, a sample of thickness  $d$  is placed between two horn antennas, and the scattering transmission coefficient,  $S_{21}$ , and phase,  $\varphi$ , are measured by the network analyzer. The process is repeated by removing the sample, and the difference between the measured quantities is used to compute the values of the dielectric constant [17–19], given by the following equations:

$$\varepsilon' = \left[ 1 + \frac{\Delta\phi}{360d} \frac{c}{f} \right]^2 \quad (10)$$

$$\varepsilon'' = \frac{\Delta A}{8.686\pi d} \frac{c}{f} \sqrt{\varepsilon'} \quad (11)$$

where  $\Delta A = 20 \log |S_{21}|$  is the attenuation of the incident microwave signal by the dielectric absorber, and  $\Delta\phi$  is the phase shift in degrees and can be computed as  $\Delta\phi = \varphi - 2\pi \cdot n$ . To find the integer  $n$ , we computed the values at two frequencies [16–20]. Figure 3, shows a free-space transmission setup to measure the attenuation and phase shift for dielectric characterization of the sample (rice-husks).

Figure 4 shows the real part ( $\varepsilon'_r$ ) of the complex permittivity ( $\varepsilon_r$ ) of two multi-layer absorbers as measured by using the free-space transmission technique. In the free-space method, the whole surface of the target is exposed to the incident wave, and the bulk properties of the target also affect the results. The non-uniform distribution of the constituents in the mixture results in impedance gradients and

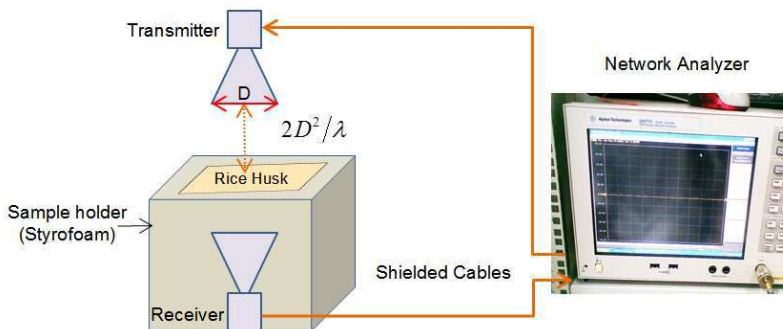


**Figure 3.** Typical free-space transmission coefficient measurement setup for dielectric characterization of the rice-husk absorber.

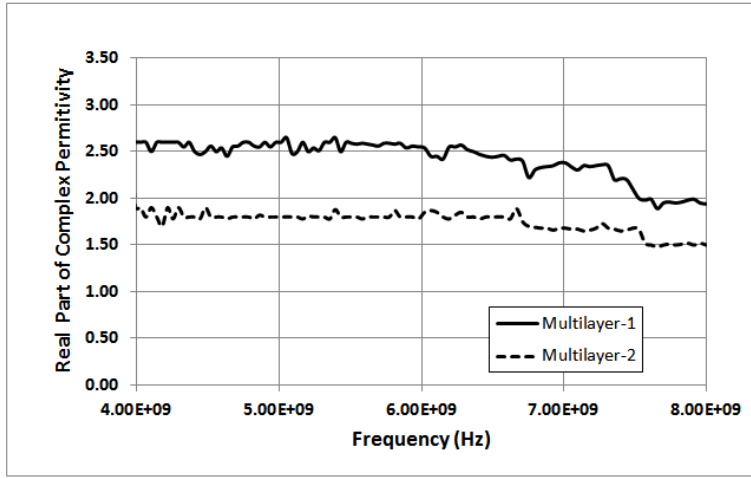


**Figure 4.** Real part of complex permittivity of two multi-layer, rice-husk microwave absorbers.

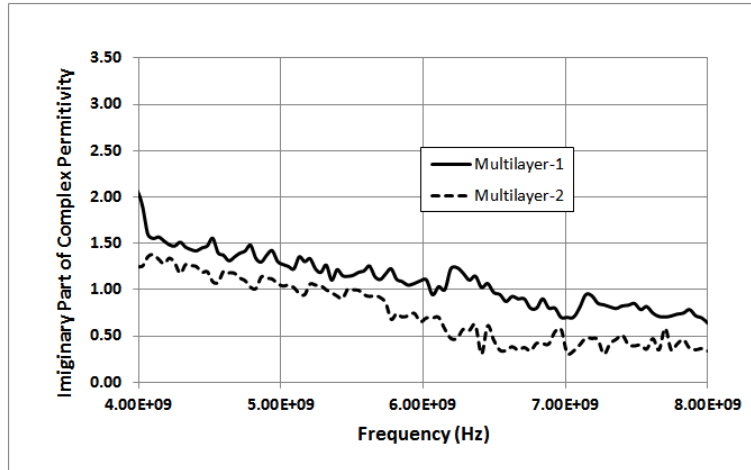


**Figure 5.** Imaginary part of complex permittivity of two multi-layer, rice-husk microwave absorbers.

causes reflections, as shown in the results. The real part of the complex permittivity controls the electrostatic energy storage capability and the speed of the incident microwave signal within the dielectric material. Figure 5 shows the imaginary part ( $\epsilon_r''$ ) of the relative complex permittivity of the two multi-layer absorbers, relating the losses offered

by the dielectric material. Usually, complex permittivity is expressed without subscript “ $r$ ” as  $\varepsilon = |\varepsilon| e^{-j\delta}$ , where  $\delta$  is the loss angle that is related to another important factor, i.e.,  $\tan(\delta) = \frac{\varepsilon''}{\varepsilon'}$ , which describes the dielectric properties.

### 3.2. Radar Cross-Section Method

The radar cross-section (RCS) method has been used to evaluate the reflectivity performance of the fabricated absorbers, and the setup is shown in Figure 6. In this method, a reference is calibrated by exposing a metallic surface to a transmitting antenna, and the signal that is reflected from the metal is measured by another antenna as a receiver. Then, the absorber being tested was placed on the reference surface, and reflection was measured again. The reflected signal from the absorber backed by a reference sample gives the reflectivity of the absorber relative to the reference. An iron-based, metallic plate was used as the backing plate, because, in most cases, large anechoic chambers are built by high permeability mild steel (MS) or galvanized iron (GI) instead of using non-magnetic sheets. The ferromagnetic nature of the iron-based enclosures with smaller sheet thickness also makes their use possible in low-frequency, magnetic shielding. However, other materials, including aluminum and copper, were also investigated in this study. The RCS method requires special testing requirements and sample size with respect to the incident wavelength to avoid edge reflections. In this study, we used a large absorber on the back of the metal back plate to focus the entire reflected signal towards the receiving antenna.



**Figure 6.** Reflectivity measurements of the graded-impedance, rice-husk microwave absorber inside the anechoic chamber by the RCS method. (a) Perforated design. (b) Non-perforated design.

### 3.3. EMI Noise Reduction

The experiment was performed inside the specially-designed, shielded anechoic chamber to avoid any unintentional noise coupling to the experimental setup. High-frequency, low-loss, shielded cables were used to minimize the attenuation of the signal and external interference. The distance from the noise source to the receptor plays an important role in noise coupling, so longer shielded cables were used to isolate the measurement system. Shielded cables are usually immune to incident electric-field noise [5], provided that they are well grounded. Signal loss introduced by lengthy cables can be compensated by increasing the signal level or by using higher-gain antennas. Noise decoupling was ensured because cables, printed circuit board (PCB) tracks, and internal wiring could behave as antennas in the electronic hardware, resulting in unintentional coupling of electromagnetic fields [19]. The metallic supports used to mount the antennas also were covered by the absorber to avoid reflections, as shown in Figure 6.

### 3.4. Calibration of the System

In this experiment, an Agilent Network Analyzer E5071C was used and Figure 7 shows the Network Analyzer before and after two-port TRL calibration. The reference plane of Network Analyzer changes with the addition of any test fixture or any device under test (DUT). Installation of any piece of coaxial cable, any coax-rectangular adaptor,



**Figure 7.** Network analyzer for characterization of the EMC of the rice-husk microwave absorber. (a) Before calibration. (b) After two-port calibration.

or any other type of adaptor or antenna at any port causes reflections and disturbs the calibration. To eliminate the effect of the test fixture or DUT, different techniques are used [21], e.g., thru-reflect-line (TRL), short-open-load-thru (SOLT), time gating, and de-embedding. The calibration of the Network Analyzer required calibration probes or kits, impedance-matched coaxial cables, and calibration standards. However, in time gating, no calibration kit is used, and the Network Analyzer is operated in the time domain so reflections could be analyzed and eliminated.

Due to the unavailability of a time gating option in the E5071C Network Analyzer, TRL calibration was performed in this study. TRL is a calibration technique in which three standards, i.e., zero-length through (T), open or short reflect (R), and line standards, are used to calibrate the Network Analyzer [22].

#### 4. ABSORBER DESIGN AND GEOMETRICAL DETAILS

The pyramidal design is the conventional design at high frequencies for microwave absorbers. This absorber design, in which the thickness of the pyramids is at least several wavelengths, offers very good performance at high microwave frequencies. At low frequencies there are wider-angle reflections, but, due to the availability of more-directional antennas at higher frequencies, the levels of the wide-angle reflections can be controlled [23]. To improve the performance of the absorber, different materials can be used, such as using added tire dust [24], split-ring resonators (SRR) [25–27], electronic band gaps (EBG) [28], and photonic band-gap (PBG) structures [29].

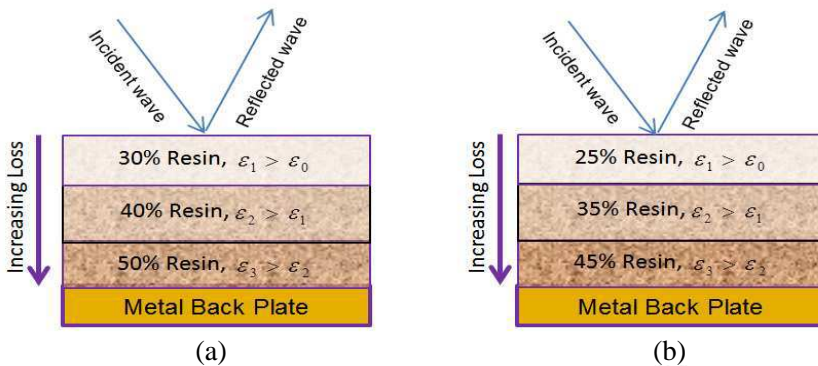


**Figure 8.** Graded impedance microwave absorbers. (a) Multilayer-1. (b) Multilayer-2.

Non-perforated and perforated designs were investigated in this study. These two designs consist of three layers of the rice-husk material with different dielectric properties. Dielectric grading of the designed absorbers was achieved during the fabrication phase by varying the polyester resin content. Multilayer-1 consisted of three layers of rice husk that were 5 mm thick and consisted of 30%, 40%, and 50% of resin by weight, whereas 25%, 35%, and 45% of resin by weight was used in multilayer-2. Figure 8 shows the multi-layer scheme for two multi-layer, rice-husk absorbers. The resin was mixed manually at room temperature before adding an organic peroxide, methyl ethyl ketone peroxide (MEKP) which is widely used for curing unsaturated polyester resins in polymer industry.

The same fabrication process was used for two perforated absorbers, i.e., Perforated-1 and Perforated-2. In the perforated designs, an array of circular holes was used to investigate the EMC

**Table 1.** Geometrical details of the impedance-graded, rice-husk microwave absorbers.

Designed Absorbers	Length (mm)	Width (mm)	Average Thickness (mm)	Number of Holes	Hole-to-Hole Distance (mm)	Average Hole Size (mm)
Multilayer -1	300	250	15	-	-	-
Multilayer -2	300	250	15	-	-	-
Perforated -1	220	220	15	59	25	3
Perforated -2	220	220	15	59	25	3

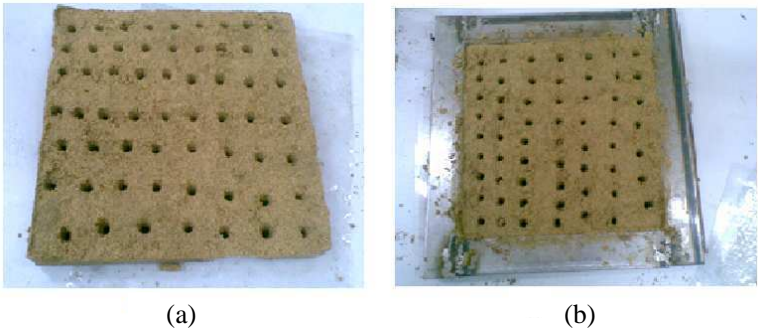


**Figure 9.** Fabricated rice-husk-based microwave absorbers. (a) Perforated-1 after fabrication. (b) Perforated-2 inside the mold during the fabrication process.

performance. The average size of each hole was 10 times less than the lowest working wavelength (at 8 GHz) to minimize the transmission of the incident microwaves through the holes. These holes were similar to an array of dielectric circular waveguides having a length that was five times the diameter of the waveguide. Both perforated absorbers had a thickness of 15 mm, which was less than the previously-designed pyramid absorber [3, 25]. Figure 9 shows the two perforated, rice-husk microwave absorbers with circular holes. Table 1 shows the geometrical details of the four absorbers that were designed. Thickness was measured at four points on each side of the absorber, and the average of all four sides was used.

## 5. RESULTS AND DISCUSSION

Experimental results for the reflectivity of the perforated and non-perforated, multiple-layer, planar, rice-husk microwave absorbers were obtained. It is a common practice to use metallic enclosures for electromagnetic attenuation, and different standards are available for their testing across a broad range of frequencies [30–33]. Microwave absorbers also can be characterized in terms of their shielding effectiveness [34], but, for the most part, their performance is described by their reflectivity with respect to a reference metallic plate.

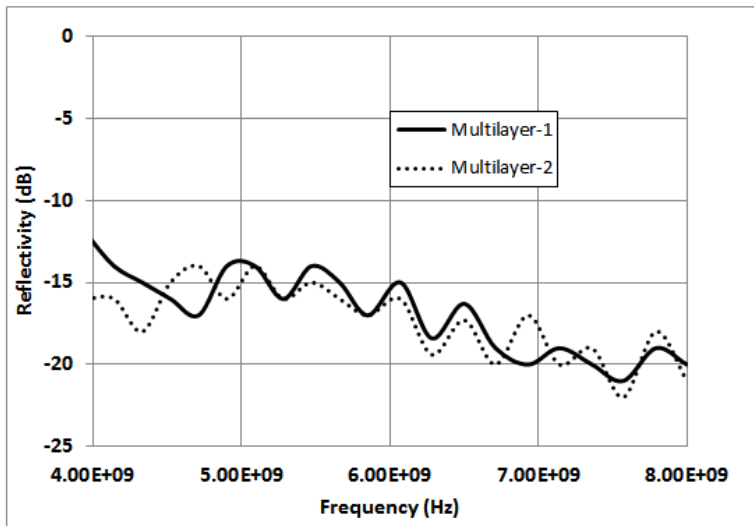


**Figure 10.** Reflectivity performance of the multi-layer, graded-impedance, rice-husk microwave absorbers at a normal incident angle.

### 5.1. Reflectivity Performance of Rice-husk Microwave Absorber

The reflectivity performances of graded-impedance, rice-husk microwave absorbers with reference to a metallic plate were measured. Figure 10 shows the reflectivity performance of Multilayer-1 and Multilayer-2 impedance-graded, rice-husk absorbers for a normal incident angle. These results were obtained by using the RCS method, as shown in Figure 6. The two absorbers that were fabricated had the same geometrical dimensions ( $30 \times 25$  cm), because, in the RCS method, the target size with respect to the incident wavelength and aperture plays the main role [35].

The results show that both absorber designs have good reflectivity performance, i.e., less than  $-10$  dB over the frequency range of 4–8 GHz. The average variation in the normal reflectivity performance of the two absorbers in the frequency range of 5–8 GHz was  $\pm 2$  dB. However, in the frequency range of 4–5 GHz, the variation was approximately  $\pm 3$  dB. These small variations were due to the difference in the compositions of the rice husks and the resin in the absorbers. However, these variations were relatively insignificant, and both absorbers exhibited good performances ( $< -10$  dB). The best

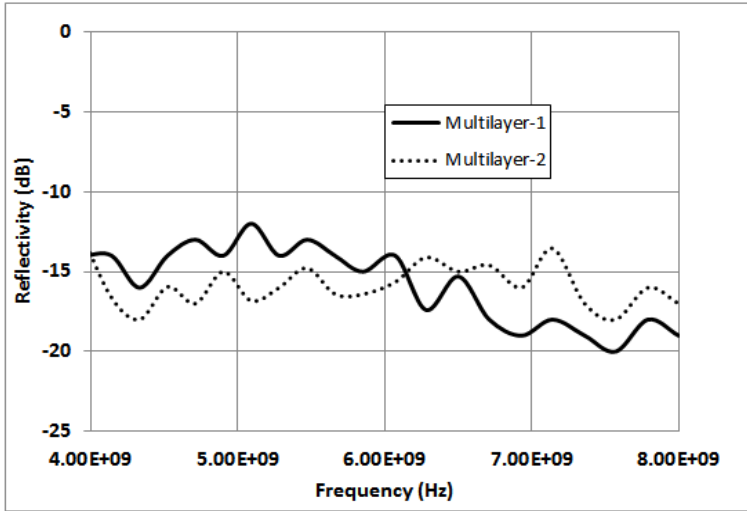


**Figure 11.** Reflectivity performance of the multi-layer, graded-impedance, rice-husk microwave absorbers at  $60^\circ$  off the normal incident angle.



**Table 2.** Average reflectivity performance of two multi-layer, impedance-graded, rice-husk microwave absorbers at normal ( $0^\circ$ ) and at  $60^\circ$  off the normal incident angle.

Frequency (GHz)	Multilayer-1		Multilayer-2	
	$0^\circ$	$60^\circ$	$0^\circ$	$60^\circ$
4	-12	-14	-16	-14
5	-14	-13	-15	-16
6	-15	-14	-16	-16
7	-20	-19	-18	-16
8	-20	-19	-21	-18
Average (4–8 GHz)	-16	-15	-17	-16

performance was obtained at high frequencies for which the ratio of wavelength to target size had the smallest values.

Figure 11 shows the reflectivity performance of both multi-layer, rice-husk microwave absorbers, when angle of incidence was 60 degree from the normal. The results show that both absorbers had good wide-angle reflectivity performance ( $< -10$  dB) even at 60 from the normal. Both absorbers had variations of  $\pm 3$  to  $\pm 4$  dB at some frequencies. However, as shown in Table 2, the average of the reflectivity performance was within  $\pm 1$  dB. In the RCS method of reflectivity measurement, the sample is placed on the reference metal plate thus, edge diffractions can cause serious errors at angles that deviate extensively from the normal angle.

Also, Table 2 shows that the high-frequency performance of the graded-impedance, rice-husk microwave absorbers was better than performance at lower frequencies. At higher frequencies (lower wavelengths) for which the ratio of thickness to incident wavelength is greater, the wave dissipates most of its energy during its passage through the material.

## 5.2. Effect of the Back Plate

Three types of reference metal plates, i.e., copper, aluminum, and iron, were investigated, and the results are shown in Figure 12. All the reference metallic plates had the same dimensions ( $30 \times 30$  cm). The results show that copper and aluminum had the same reflectivity performance in the frequency range of 4.5–5.5 GHz, but, at higher frequencies, the performance was within  $\pm 2$  to  $\pm 3$  dB. Reflectivity of

the iron was 2–3 dB greater than that of copper and aluminum in the frequency range of 4.4–5.8 GHz. At frequencies above 5.8 GHz, the reflectivity of the iron decreased and was comparable to the reflectivity of aluminum, except at the frequencies of 6.2 GHz and 7.6 GHz. However, copper had greater reflectivity than either aluminum or iron in the frequency range of 5.9 GHz to 8 GHz. Reflection of the microwaves by the target depends on the impedance mismatch at the interface of the two media.

Copper and aluminum are non-magnetic ( $\mu_r = 1$ ) materials, but iron is a magnetic material with a relative magnetic permeability  $\mu_r > 1$ . Conductors are considered as perfect reflectors of microwaves, but their reflectivity depends on their conductivity [36]. The conductivity of copper is greater than that of aluminum and iron, so it must have large reflections. The presence of impurities in the metals affects their conductivity and hence their reflectivity. Iron has a strong tendency to corrode readily in moist environment, as compared to the copper and aluminum. In EMC applications, where iron is used as an electromagnetic shield, corrosion is controlled by measures such as alloying, painting, or galvanizing with zinc. Corrosion affects the reflection characteristics as well as the shielding effectiveness of the iron by producing an insulating layer on its surface. The non-uniform distribution of the corrosion reduces the reflection performance of the iron further at higher frequencies.

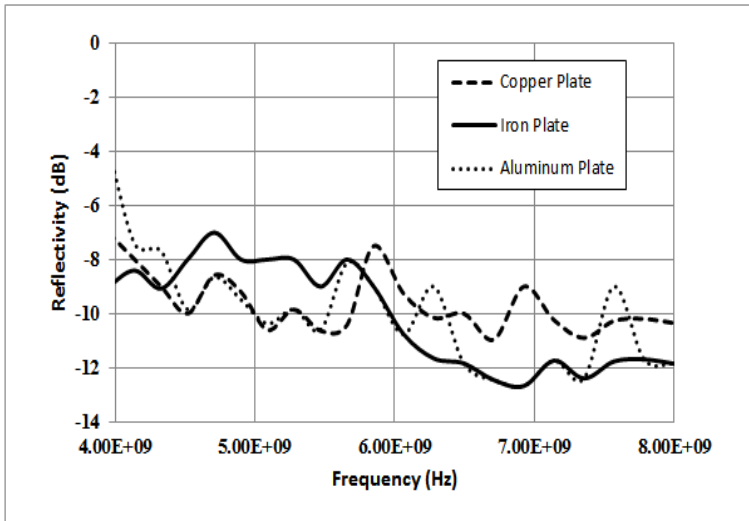


**Figure 12.** Reflection loss of different reference metal plates.

### 5.3. Effect of Perforation

Figure 13 shows the reflectivity performance of the rice-husk, Perforated-1 microwave absorber over the frequency range of 4–8 GHz. The absorber's reflectivity performance was better than  $-10$  dB at normal and  $60^\circ$  off the normal incident angle. In the frequency range of 5.3–8.0 GHz, the performance was better than  $-15$  dB, and it increased with frequency. The best performance was obtained at normal and at  $45^\circ$  off the normal incident angle at higher frequencies. There is a decrease in reflectivity performance for  $60^\circ$  off the normal at higher frequencies due to the leakage caused by edge reflections. The rice-husk microwave absorber had 3-mm circular holes, but the size of the holes was very small compared to the working wavelength (10 times smaller).

There is a periodic mismatch of impedance and a discontinuity in the dielectric properties of the rice-husk material due to the presence of holes. These periodic holes behave like multiple scattering centers and cause reflections, as shown in the Figures 13 and 14.

The reflectivity performance of the rice-husk, Perforated-2 microwave absorber is shown in Figure 14. There was a decrease in performance at  $60^\circ$  off the normal, but the overall performance was better than  $-10$  dB. The best performance was obtained at the high-frequency end for a normal angle of incident. A maximum variation

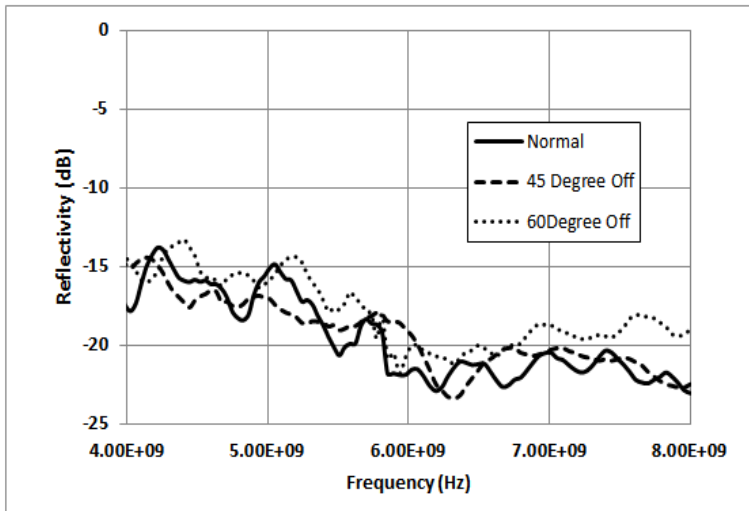


**Figure 13.** Reflectivity performance of the rice-husk, microwave, Perforated-1 absorber.

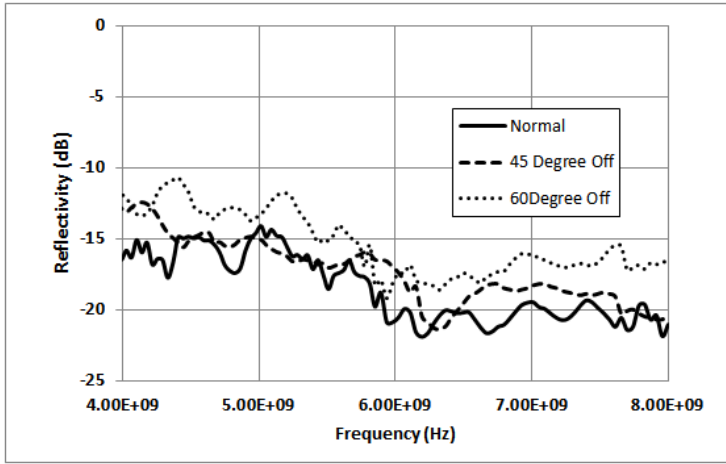


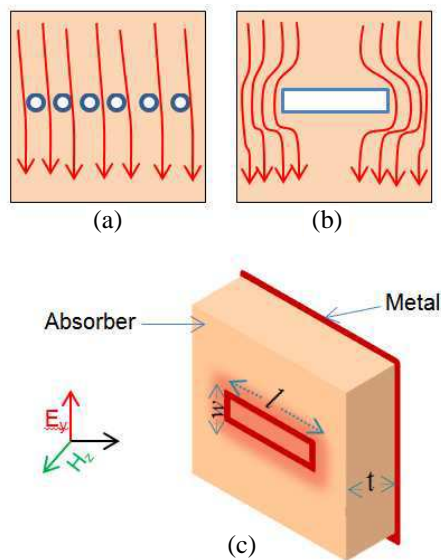
**Figure 14.** Reflectivity performance of the rice-husk, microwave, Perforated-2 absorber.

of 4 dB was observed in the performance of both absorbers in the frequency range of 4.0–5.8 GHz at 60° off the normal incident angle. Reflectivity performance of both absorbers was comparable for the normal incidence angle.

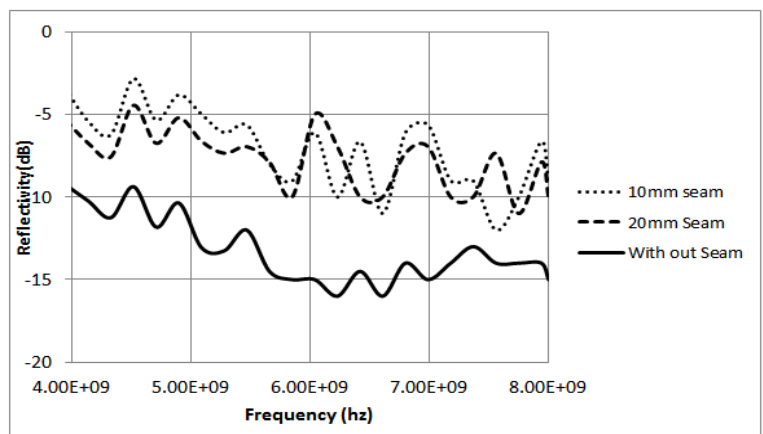
#### 5.4. Effect of Seams

Figure 15 shows the alignment of the induced current lines within the absorbing material due to the presence of an array of holes and a seam. In this experiment two seams were investigated and the electric-field component of the microwave signal was oriented perpendicular to the seams. The seams were generated by placing the two pieces of the same rice-husk absorber at 10 mm and 20 mm apart. A seam is actually a long narrow slot that may or may not have electrical contact at various points along its length. When electromagnetic signal interacts with the seam having length  $l$ , it behaves like a radiating source whose complement is a long wire that looks like a dipole. The length of the slot represents the length of the equivalent complementary dipole and if the length is of the order of  $\lambda/2$  then it will become an efficient antenna. Therefore in EMC applications, a single lengthy seam is avoided and a linear array of closely spaced apertures or holes is preferred.

Figure 16 presents the degradation of the reflectivity performance of the absorber due to the presence of long seams. The results presented in Subsection 5.3 also confirm the better reflectivity performance of array of closely spaced holes in perforated absorbers.



**Figure 15.** (a) Current distribution due to an array of circular holes. (b) Current distribution due to a single slot. (c) Rice-husk microwave absorber with a seam of  $w = 10$  mm, 20 mm,  $l = 200$  mm and  $t = 15$  mm.



**Figure 16.** Reflectivity performance of the rice-husk, microwave absorber with 10-mm and 20-mm seams.

High-frequency, incident waves can pass through the seam easily and cause reflections from the metal back plate. The results showed

large reflections for both seams, especially at high frequencies (5.9–8.0 GHz). The presence of the seams created an impedance mismatch and a discontinuity in the dielectric properties of the material at seam’s positions. The results showed a reflectivity difference of  $\pm 2$  dB to  $\pm 3$  dB between the two seams. Without the seams, the reflectivity performance of the rice-husk, microwave absorber was better ( $\leq 9$  dB) than the reflectivity performance of both seams in the frequency range of 4.0–8.0 GHz. At low frequencies, there was a performance degradation of 4.0–5.0 dB due to the effects of the seams. However, in the frequency range of 5.8 to 7 GHz, the largest performance degradation of 5–10 dB was observed due to the large reflections.

6. COMPARISON OF REFLECTIVITY PERFORMANCE

Table 3 shows the reflectivity performance of the graded-impedance, rice-husk, microwave absorbers along with a commercially available flat absorber (LF-74). In this study, four impedance-graded, microwave absorbers were fabricated by using rice husks, polyester, and MEKP hardener. LF-74 is a member of C-RAM LF, a series of lightweight radar absorbers made from graded layers of lossy, open-cell, plastic foam [37]. Designed absorbers were also investigated for 45° oblique angle reflectivity performance. Average results for oblique angle reflectivity performance of two multilayers and perforated absorbers are also presented for comparison. All the designed impedance-

**Table 3.** Performance comparison of rice-husk, microwave absorbers with a commercially available (19.1 mm) absorber over the frequency range of 4–8 GHz.

Frequency (GHz)	15-mm-thick Fabricated Rice Husk Absorbers							LF-74
	Non-Graded	Average per formance at oblique an gle (45°)		Performance at normal angle				
		Multilayers	Perforated	Multilayer-1	Multilayer-2	Perforated-1	Perforated-2	
4	-9	-10	-13	-12	-16	-17	-16	-20
5	-8	-13	-16	-14	-15	-15	-15	
6	-10	-17	-19	-15	-16	-22	-21	
7	-9	-18	-19	-20	-17	-21	-19	
8	-9	-18	-21	-20	-21	-23	-22	
Average (4-8 GHz)	-9	-15	-17	-16	-17	-19	-18	

graded, rice-husk absorbers had good (less than  $-10$  dB) results in the range of 4–8 GHz even at oblique angle. The performance also was comparable to the LF-74 microwave absorber, especially at the higher-frequency end. However, the fabricated rice-husk, microwave absorbers had minimum (but less than  $-10$  dB) performance at lower frequencies. Multilayer-1 had its worst performance at 4 GHz, but, at higher frequencies, its performance was comparable to that of the others. The difference in the performance was due to the fact that the LF-74 absorber was thicker (19.1 mm) than the rice-husk absorbers. Table 3 also confirms the better performance of graded impedance, microwave, rice-husk absorbers as compared to the non-graded, rice-husks based microwave absorber.

## 7. CONCLUSIONS

In this paper, we have described the graded-impedance method that was used to fabricate rice husk-based, microwave absorbers. We conducted an experimental investigation of the performance of the rice-husk material to determine its viability for use in future EMC solutions. The experimental results showed that the impedance-graded, rice-husk material in planar geometry also can be used efficiently at low frequencies to provide an anechoic environment. Two designs were investigated, i.e., the impedance-graded, multi-layer design and the perforated design, and the results showed that their performances were better than  $-10$  dB. This means that the proposed absorbers can absorb more than 90% of the incident microwave energy. Comparisons with a commercially-available absorber also confirmed the effectiveness of the impedance-graded, rice-husk material as a good microwave-absorbing candidate for future EMC applications. These absorbers could be a very wise choice for small EMC chambers for which size is the main constraint. The prospective future applications of the perforated, rice-husk, microwave absorber may include the lining of the metallic honeycombs that are used for ventilation in shielded anechoic chambers. In future research, these absorbers should be investigated for temperature effects, electrical stresses, airflow through perforated absorbers, and high-power microwave exposures.

Usually agricultural waste is burned, which increases the percentage of  $\text{CO}_2$  in the atmosphere. The use of rice-husk material as a renewable energy source in the microwave industry certainly could decrease the harmful ecological contribution (black carbon) of this material. Large-scale production of rice husk-based microwave absorbers also will provide a cheaper microwave anechoic source.

## REFERENCES

1. Kartini, K., H. B. Mahmud, and M. S. Hamidah, "Absorption and permeability performance of Selangor rice husk ash blended grade 30 concrete," *Journal of Engineering Science and Technology*, Vol. 5, No. 1, 1–16, 2010.
2. Jain, A. K., S. K. Sharma, and D. Singh, "Reaction kinetics of paddy husk thermal decomposition," *IECEC-96*, Vol. 4, 2274–2279, 1996, 0-7803-3547-3-7/16.
3. Nornikman, H., F. Malek, P. J. Soh, A. A. H. Azremi, F. H. Wee, and A. Hasnain, "Set up and results of pyramidal microwave absorbers using rice husks," *Progress In Electromagnetics Research*, Vol. 111, 141–161, 2011.
4. Chung, B. K. and H. T. Chuah, "Modeling of RF absorber for application in the design of anechoic chamber," *Progress In Electromagnetics Research*, Vol. 43, 273–285, 2003.
5. Schmitt, R., *Electromagnetics Explained: A Handbook for Wireless/RF, EMC, and High-speed Electronics*, Elsevier Science, USA, 2002.
6. Morgan, D., *A Handbook for EMC Testing and Measurement*, Peter Peregrinus, London, United Kingdom, 1994.
7. Sasagawa, T., O. Hashimoto, S. Watanabe, T. Saito, and H. Kurihara, "Examination on temperature distribution of a pyramidal EM-wave absorber under high power injection," *Proceedings of Asia-Pacific Microwave Conference*, 2007.
8. Ali, I. A. and L. J. Auchterlonie, "Temperature distribution in uniform and layered microwave absorbers in waveguide," *IEE Proc.*, Vol. 130, No. 3, 1983.
9. Ott, H. W., *Electromagnetic Compatibility Engineering*, John Wiley & Sons, Inc., Hoboken, New Jersey, 2009.
10. Pozer, D. M., *Microwave Engineering*, 3rd Edition, John Wiley & Sons, 2005.
11. Tong, X. C., *Advanced Materials and Design for Electromagnetic Interference Shielding*, CRC Press, Taylor & Francis Group, Broken Sound Parkway NW, Suite 300, Boca Raton, 2009.
12. Kumar, S. B., U. Raveendranath, P. Mohanan, K. T. Mathew, M. Hajian, and L. P. Ligthart, "A simple free-space method for measuring the complex permittivity of single and compound dielectric materials," *Microwave and Optical Technology Letters*, Vol. 26, No. 2, Jul. 2000.
13. Helme, B. G., "Measurements of the microwave properties of



- materials,” *IEEE Colloquium on Industrial Uses of Microwaves*, 1–7, 1990.
14. Williams, N., V. K. Varadan, D. Ghodgaonkar, and V. V. Varadan, “Measurement of transmission and reflection of conductive lossy polymers at millimeter-waves frequencies,” *IEEE Transaction on Electromagnetic Compatibility*, Vol. 32, No. 3, 236–240, Aug. 1990.
  15. Barker-Jarvis, J., et al., “Dielectric characterization of low-loss materials-A comparison of techniques,” *IEEE Trans. Dielectric. Electr. Insul.*, Vol. 5, No. 4, 571–577, Aug. 1998.
  16. Trabelsi, S. and S. O. Nelson, “Calibration methods for nondestructive microwave sensing of moisture content and bulk density of granular materials,” *Transactions of the ASAE*, Vol. 47, No. 6, 1999–2008, 2004.
  17. Trabelsi, S. and S. O. Nelson, “Nondestructive sensing of bulk density and moisture content in shelled peanuts from microwave permittivity measurements,” *Food Control*, Vol. 17, 304–311, Elsevier, 2006.
  18. Trabelsi, S., A. W. Kraszewski, and S. O. Nelson, “Phase-shift ambiguity in microwave dielectric properties measurements,” *IEEE Transactions on Instrumentation and Measurement*, Vol. 49, No. 1, Feb. 2000.
  19. Williams, T., *EMC for Product Designers*, 3rd edition, United Kingdom, 2001.
  20. Jose, K. A., V. V. Varadan, and V. K. Varadan, “Free-space vs. one horn interferometer techniques for radar absorber measurements,” *Microwave Journal*, 1998.
  21. Rolfes, I. and B. Schiek, “Calibration methods for microwave free space measurements,” *Advances in Radio Science* 2, 19–25, 2004.
  22. “Agilent network analysis applying the 8510 trl calibration for non-coaxial measurements,” Product Note 8510-8A.
  23. Chung, B. K. and H. T. Chuah, “Design and construction of a multipurpose wideband anechoic chamber,” *IEEE Antennas and Propagation Magazine*, Vol. 45, No. 6, Dec. 2003.
  24. Malek, F., E. M. Cheng, O. Nadiyah, H. Nornikman, M. Ahmed, M. Z. A. A. Aziz, A. R. Othman, P. J. Soh, A. A. H. Azremi, A. Hasnain, and M. N. Taib, “Rubber tire dust-rice husk pyramidal microwave absorber,” *Progress In Electromagnetics Research*, Vol. 117, 449–477, 2011.
  25. Nornikman, H., B. H. Ahmad, M. Z. A. A. Aziz, F. Malek, H. Imran, and A. R. Othman, “Study and simulation of an edge

- couple split ring resonator (EC-SRR) on truncated pyramidal microwave absorber,” *Progress In Electromagnetics Research*, Vol. 127, 319–334, 2012.
26. Ren, L. S., Y. C. Jiao, J.-J. Zhao, and F. Li, “RCS reduction for a fss-backed reflector using a ring element,” *Progress In Electromagnetics Research Letters*, Vol. 26, 115–123, 2011.
  27. Lee, H. M. and H. S. Lee, “A dual band metamaterial absorber based with resonant-magnetic structures,” *Progress In Electromagnetics Research Letters*, Vol. 33, 1–12, 2012.
  28. Elsheikh, D. N., H. A. Elsadek, E. A. Abdallah, M. F. Iskander, and H. Elhenawy, “Ultra wide bandwidth umbrella-shaped micro strip monopole antenna using spiral artificial magnetic conductor (SAMC),” *IEEE Antennas and Wireless Propagation Letters*, Vol. 8, 1255–1258, 2009.
  29. Yiqiang, W. and F. Tao, “The study on a patch antenna with PBG structure,” *Third International Symposium on Intelligent Information Technology Application*, Vol. 3, 565–567, 2009.
  30. Hemming, L. H., *Electromagnetic Anechoic Chambers a Fundamental Design and Specification Guide*, IEEE Press, Wiley-Interscience, 2002.
  31. Hemming, L. H., *Architectural Electromagnetic Shielding Handbook*, IEEE Press, New York, 1992.
  32. IEEE 299–1997, “IEEE standard method of measuring the effectiveness of electromagnetic shielding enclosures,” 1997.
  33. NSA 94-106, *National Security Agency Specification for RF Shielded Enclosures: General Specifications*, Oct. 24, 1994.
  34. Koledintseva, M. Y., A. G. Razmadze, A. Y. Gafarov, V. V. Khilkevich, J. L. Drewniak, and T. Tsutaoka, “Attenuation in extended structures coated with thin magneto-dielectric absorber layer,” *Progress In Electromagnetics Research*, Vol. 118, 441–459, 2011.
  35. Hiatt, R. E., et al., “A study of VHF absorbers and anechoic rooms,” Report 5391-I-f, University of Michigan, Feb. 1963.
  36. Zhou, L., W. Wen, C. T. Chan, and P. Sheng, “Reflectivity of planar metallic fractal patterns,” *Applied Physics Letters*, Vol. 82, Feb. 17, 2003.
  37. “C-Ram LF and LF-W flexible foam sheet broadband microwave absorber,” Technical Bulletin 320-1, 2008, [www.cumingmw.com](http://www.cumingmw.com), Document Control No. N-07-000-01353-3.